Injectable Rosette Nanotube Nanomatrix for Localization of Bioactive Protein for Growth Plate Repair

By

Peter Lam

B.S., Worcester Polytechnic Institute, 2015

Thesis

Submitted in partial fulfillment of the requirements for the Degree of Master of Science in the Department of Biomedical Engineering at Brown University

PROVIDENCE, RHODE ISLAND

MAY 2017

AUTHORIZATION TO LEND AND REPRODUCE

As the sole author of this thesis, I authorize Brown University to lend it to other institutions or individuals for the purpose of scholarly research.

Date:_____ Signature:_____
Peter Lam, Author

I further authorize Brown University to reproduce this thesis by photocopying or other means, in total or in part, at the request of other institutions or individuals for the purpose of scholarly research.

Date:_____ Signature:_____
Peter Lam, Author

This thesis by Peter Lam is accepted in its present form by the Department of Biomedical Engineering as satisfying the thesis requirements for the degree of Master of Science

Date:_____ Signature:_____
Dr. Yupeng Chen, Advisor

Date:_____ Signature:_____
Dr. Jacquelyn Schell, Reader

Date:_____ Signature:_____
Dr. Eric M. Darling, Reader

Approved by the Graduate Council

Date:_____ Signature:_____
Dr. Andrew G. Campbell, Dean of Graduate School

Acknowledgements

I would like to acknowledge Dr. Yupeng Chen for giving me the opportunity to conduct my Master's research at the laboratory in the Department of Orthopaedics at the Rhode Island Hospital. I appreciate his support and mentorship throughout the project. I would also like to thank Dr. Qian Chen and Dr. Michael Ehrlich for their expertise in the field and advice on the research. I express my appreciation to Dr. Hongchuan Yu for synthesizing the rosette nanotubes to use in my experiments. I would also like to thank all the collaborators that contributed to the project. Next I want to acknowledge Brandon Vorrius for training me on various lab techniques used in my research. Finally, I would like to thank Dr. Jacquelyn Schell and Dr. Eric Darling for being readers for my thesis.

Table of Contents

List of Figures

Abstract

Growth plate fracture is a serious injury that affects children and adolescents. These types of fractures can occur from physical sports, a fall or from overuse. The most common growth plate fractures occur in the phalanges or in the bones in the lower area of the leg such as the tibia and fibula. These fractures can lead to uneven bone growth and bone deformity if left untreated due to bony bridge formation in the cartilage area. The current treatments for growth plate fractures involve immobilization or surgery, depending on the severity of the injury. Surgery involves the removal of the bony bridge and implantation of autologous fat tissue or screws to discourage further bony bridge formation. The disadvantage of surgery is that it is very invasive and is often unsuccessful. Therefore, there is a need for a better therapy to treat growth plate fractures.

This study explores a novel therapy using a nanomatrix made up of rosette nanotubes and matrilin-3 to treat growth plate fractures. The aim of this study is to characterize the nanomatrix as well as assess its efficacy *in vivo*. The results indicate the delivery of matrilin-3 in a matrix with rosette nanotubes is able to sustain the protein inside the injury site longer to prolong its therapeutic effect. Moreover, the results assessing the efficacy of the nanomatrix indicate improved healing of the growth plate fracture by minimizing the degree of bone deformity.

Background

The Growth Plate

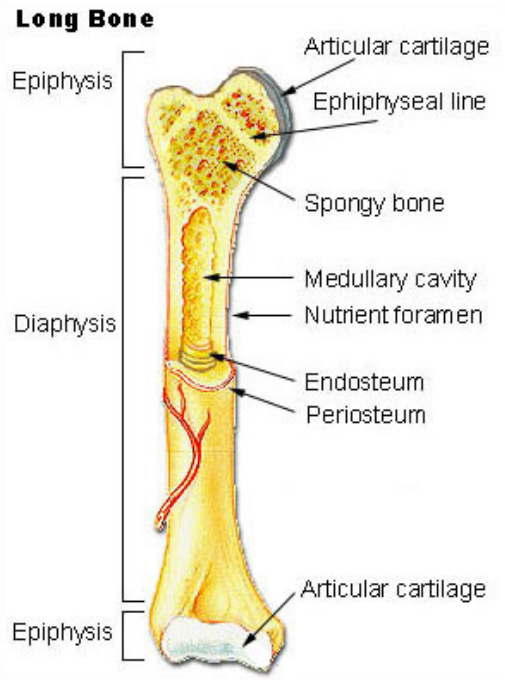

Figure 1. Anatomy of the long bone (1).

The growth plate, also called the epiphyseal plate or physis, is an area of growing cartilage tissue located at the ends of the long bones in young children. There is a growth plate located at each end of the long bone and is responsible for the growth of the bone to its full length when it reaches maturity. The growth plate is replaced by solid bone when the growth is complete. The growth plate is made up of 3 zones. Each of these zones have multiple layers. The zone closest to the epiphysis, the rounded end of the long bone, is called the growth zone. This zone is made up of the germinal and proliferative layers. Longitudinal growth of the bone occurs in this zone, where cells in the germinal layer move from resting state into the proliferative layer for mitosis and division. The next zone is the zone of cartilage maturation and is made up of the hypertrophic layer and layer of calcification. Chondrocytes (cartilage cells) mainly resides in this zone and is enlarged in the hypertropic layer. These cells disintegrate and form a layer of necrotic calcified cells that develop a network of tunnels to allow for osteoblasts and

metaphyseal vessels to infiltrate. This zone is the weakest part of the growth plate and is especially prone to injury. However, half of the growth plate fractures occur across multiple zones. The final area is the zone of transformation which consists of 2 layers. They are the layer of ossification and the layer of vascular penetration. Vessels penetrate into the layer of calcified chondrocytes in the layer of calcification and osteogenesis occurs in the final zone (2,3).

Growth Plate Fractures

Growth plate fractures affects many children and adolescents, as their bones are not fully developed yet. Any sort of injury to the bone can have negative effects on the growth of the bone. A majority of growth plate fractures occur in the phalanges or in the leg in the tibia and fibula. Fractures to the growth plate can be caused by numerous things, due to the weak nature of the growth plate compared to other parts of the bone. A majority of these fractures are caused by accidents that occur during physical activities and sports. Growth plate fractures can also occur on children who is experiencing abuse or exposure to extreme cold. The growth plate can be damaged from extreme cold and lead to stubby fingers and degenerative arthritis. Children with neurological disorders that causes muscular imbalances or sensory deficiency are more prone to growth plate fractures in the ankle and knee. Genetic disorders that affect musculoskeletal system can cause poorly formed or irregularly functioning growth plate and make children with these disorders more susceptible to injury. Metabolic diseases such as kidney failure and hormone disorders can also affect the functionality of the growth plate. Children who experience persistent pain should consult with their doctor to determine if they have a growth plate fracture. Doctors usually perform an x-ray to diagnose the severity of the injury. They may also perform other diagnostic tests such as magnetic resonance imaging (MRI), computed tomography (CT) , and ultrasound (4).

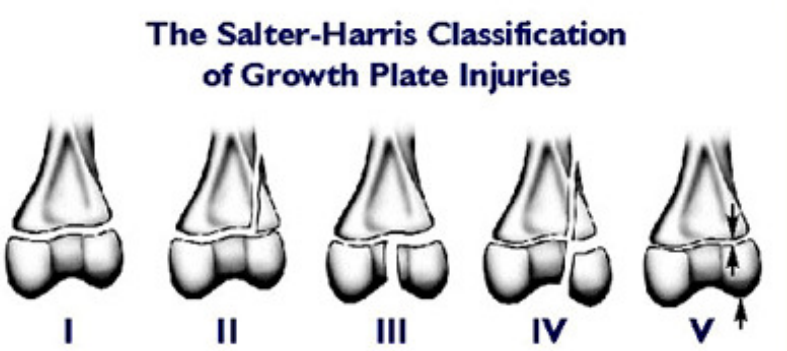

Figure 2. Illustration of the different types of growth plate fractures using the Salter-Harris Classification (4).

There are different types of fractures that can occur on the growth plate. Figure 2 shows an illustration of the different types of growth plate fractures. Type I fracture is classified as a fracture through the growth plate. In this type of fracture, the epiphysis is separated from the end of the long bone and the growth plate is still attached to the epiphysis. These types of fractures have good prognosis and the patient will most likely recover quickly with a low chance of requiring surgery (4). Treatment of type I fractures involve the displacement of the injury in a cast or a brace after the fracture has been put back into place (2). Type II fracture is when there is a fracture through the growth plate and the metaphysis, which is the wider area at the end of the shaft of the long bone . This type of fracture is the most common type of fracture that can occur on the growth plate. Similar to type I fractures, type II fractures can be treated by putting the fracture back into place and immobilizing it. This type of fracture also has a good prognosis for healing with a low chance of affecting the growth of the bone. Rare cases can occur that might require the need for a fixation if the displacement of the bone is severe. Type III fracture is when there is a fracture through the growth plate and epiphysis. This type of fracture rarely occurs and most of the time it affects the lower end of the tibia. Type III fractures cuts through the epiphysis completely and separates a portion of the epiphysis and the growth plate from the metaphysis(4). Surgery for this type of fracture is recommended for correct alignment followed by splintage. A

CT scan is commonly done to diagnose this type of fracture and plan for surgery(2). The prognosis for recovery is usually good if the blood supply to the affected region of the epiphysis is still intact and the joint surface heals properly. Type IV fracture occurs when there is a fracture through the growth plate, metaphysis, and epiphysis. This type of fracture commonly affects the end of the humerous, which is the bone in the upper arm near the elbow. Similar to type III fractures, surgery is required for type IV fractures to restore the joint surface to its normal state and to align the growth plate. Prognosis for growth for type IV fractures is poor unless there is perfect alignment of the growth plate and must maintain that alignment during healing. Bending of the bone can occur if alignment is not maintained. Finally, type V fracture is when there is a compression fracture through the growth plate. This type of injury is uncommon and happens when the growth plate is compressed when the end of the bone is crushed. Most occurrence of this type of fracture is seen in the knee and ankles (4). The prognosis for this fracture is poor and patients affected by it will most likely experience stunting of growth because there is direct damage to the cells in the growth plate. Treatment for type V fractures involve protected weight bearing and follow up diagnosis to determine if there is any deformity or growth interruption (2). Younger patients are more susceptible to progressive uneven bone growth or deformity because older children have a shorter amount of time left for growth. If deformity occurs, surgery may be required to correct the bones through lengthening. There is also a newer classification of growth plate fractures that has been added. The type VI fracture is when a portion of the growth plate, epiphysis, and metaphysis is missing. This occurs in open wounds or compound fractures and is often caused by farm machinery, snowmobiles, lawnmowers or gunshot wounds. Treatment for this type of fracture requires surgery and subsequent reconstructive or corrective surgery and will most likely cause stunted growth in the bone (4).

Biological Mechanism

When a growth plate fracture occurs, there is a sequence of events that happens at the injured site at the molecular level for recovery. The first step involves the inflammatory phase, which is when there is infiltration of inflammatory cells such as neutrophils, macrophages and lymphocytes into the injured growth plate. There is also an up-regulation of inflammatory cytokines and mediators at the site. Many animal models have been developed to characterize these findings and show indication of these cells and cytokines at the injured through mRNA expression of certain markers (5-7). The next step is the fibrogenic phase, which occurs between day 3 and 7 after the injury (8). During this phase, there is an infiltration of mesenchymal stems cells (MSCs) and blood vessels to the injured growth plate from the bone marrow (9,10). MSCs are cells that are able to differentiate into a number of specialized cells such as chondrocytes, osteoblasts, adipocytes, and tenocytes. These stem cells will differentiate into the different kinds of cells according to stimuli and growth factors that are present in the micro environment (11). The infiltrated MSCs have shown to express bone morphogenic proteins (BMPs) and platelet derived growth factors (6,7, 12). Studies have shown that the MSCs present at the injured growth plate show expression of the chondrogenic marker collagen-2 and osteogenic marker Runx2 (7, 8). These results suggest the presence of pre-osteoblasts, pre-chondroblasts, and osteoprogenitor cells in the influx of MSCs that infiltrates into the injured site (5). These cells could be from pre-existing cells at the site or derived from the infiltrated MSCs. The results from these studies suggest the MSCs are able to undergo chrondrogenesis, osteogenesis, and angiogenesis. The final stage of recovery is the osteogenic and remodeling phases, which usually occurs after day 7 post-injury (8). During the osteogenic phase, the MSCs differentiate into osteoblasts and show increased levels of the bone matrix protein osteocalcin (8, 13). There is also an increase in

mRNA expression of osteocalcin during the bone remodeling phase. However, there is a low expression of chondrogenesis related genes such as collagen-2a and Sox9 (6). In addition, studies have shown an increase expression of vascular endothelial growth factor (VEGF) (14). This growth factor is known to promote angiogenesis and osteogenesis, as well as osteoclast recruitment (15). The studies mentioned above indicate the formation of a bony bridge, which is undesired in the growth plate since it is made up of cartilage (5).

The main problem with growth plate fractures is the formation of the bony bridge in the growth plate due to differentiation of MSCs into osteoblasts. Studies have also shown that growth plate injury can also inadvertently affect adjacent cartilage that were not injured (16, 17). Evidence indicate a significant decrease in chondrocyte proliferation and an increase in apoptosis. There was a decrease in expression in chondrogenic factor Sox9 and growth factors compared to the control group of uninjured growth plate (17). In addition, there is an increase in expression of apoptotic marker, caspase-3 protein (18). Another problem is the process of endochondral ossification. This is the process where hypertrophic chondrocytes will become vascularized by blood vessels. Osteogenic progenitors are then recruited to the site and eventually lead to bone formation. The process is responsible for the development of bone in the early stages of life (19). Angiogenesis plays a key role in endochondral ossification and is made possible in the growth plate after an injury from evidence mentioned earlier due to the presence of VEGF (20, 21). Studies done using the rat growth plate injury model found increases in expression of bone related genes such as osteocalcin and Runx2 along with an increase in expression of collagen-10. Collagen-10 is known to be expressed by hypertrophic chondrocytes during endochondral ossification. This evidence suggest that endochondral ossification

inadvertently contribute to the bony bridge formation in the growth plate and inhibition of angiogenesis could mitigate the formation (7, 13, 22).

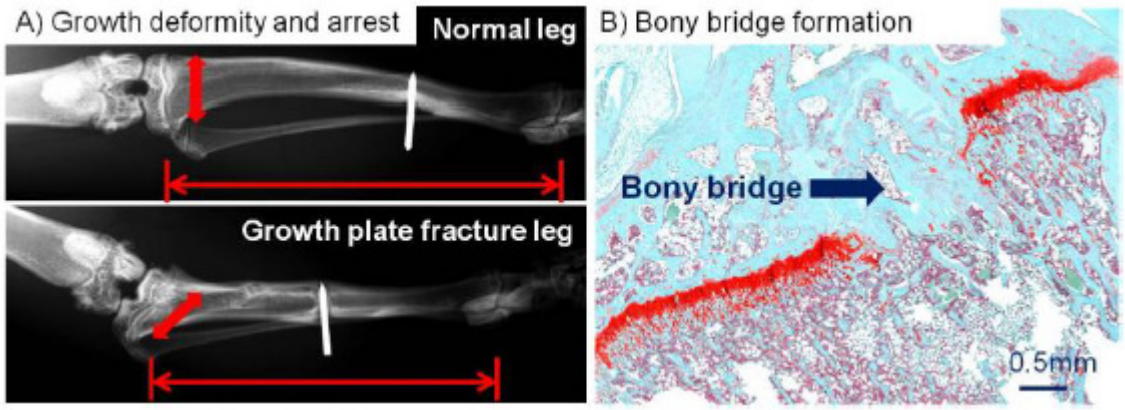

Figure 3. A) Faxitron X-ray image of rat proximal tibia before injury and 3 months post injury. Red vertical arrows indicate deformity and horizontal arrows indicate shortening of bone growth. B) Histological image of the tibia post injury showing bony bridge formation.

Significance

Currently, there is no proven biological therapy that is used to prevent the formation of the bony bridge following a growth plate fracture. The presence of the bony bridge in the growth plate results in bone deformity and uneven bone growth if left untreated. The only way to deal with the bony bridge formation is to perform corrective surgery, which includes the lengthening of the limb and implantation of biomaterials. Limb lengthening is used to correct uneven bone growth between limbs by using a scaffold to stabilize and stretch the affected limb in surgery. This procedure is invasive to the patient and requires the use of multiple pins. Complications from this procedure include infections at the site of the pins and a lengthy time for proper alignment (5). Recent advancements in this procedure utilizes an internally implanted nail but is only limited to use on adults, which is not desirable since growth plate fractures mainly affects children (23). Moreover, bone deformities are treated by implantation of interpositional materials after the surgical removal of the bony bridge. This procedure is called the Langenskiold method

and have been previously done using various materials such as muscle, fat, bone wax, bone cement, and polymeric materials (24, 25). As a result there is a need for a biological therapy that is able to prevent the bony bridge formation in the growth plate by promoting chondrogenesis for cartilage regeneration and potentially inhibit or mitigate osteogenesis and angiogenesis. There has been advances in this area to develop a therapy for this type of injury (5). Experimental work has been done to transplant chondrocytes and MSCs to the injured growth plate to promote or enhance cartilage regeneration. However, there are challenges to developing a successful therapy for this problem. Incorporation of growth factors needs to be explored to optimize cartilage regeneration at the injured growth plate and could be a tedious task to accomplish with the plethora of growth factors available. Also, an appropriate matrix support is needed for transplantation to promote chondrogenesis. Ideally, the material should be biocompatible and biodegradable and is able to promote cell adhesion for tissue growth (25-29).

This study explores the use of a novel therapy to treat growth plate fractures using a nanomatrix formed by a mixture of Matrilin-3 protein and rosette nanotubes. The idea is to inject the matrix into the injured growth plate in solution and have the materials self-assemble into a matrix inside the injury site. The goal is to use matrilin-3 to promote chondrogenesis and inhibit angiogenesis while providing a matrix with the rosette nanotubes for a sustained effect as well as provide a scaffold for cell adhesion of chondrocytes. These two materials were chosen for their beneficial properties regulating chondrogenesis.

Matrilin-3

Matrilin-3 (MATN3) is a part of a family of non-collagenous extracellular matrix proteins and is expressed in cartilage and other types of extracellular matrices. The matrilin family have 4 different members and have similar domain structures. The proteins are made up

of two von Willebrand factor A(VWA) domains that are connected by a number of epidermal growth factor domains which vary in number between the different members in the matrilin family. The subunits in the protein form trimers or tetramers through the C-terminal α-helical coiled-coil domain. Figure 4 shows an illustration of the structures of the matrilin proteins. Matrilin-3 only have one VWA domain, unlike the other 3 proteins in the family (34). Matrilin-3 is also the smallest protein in the family and is often co-expressed with matrilin-1 in cartilage (35). Studies have shown that matrilin-3 are present in the growth plate in resting, proliferating, and hypertrophic chondrocytes (36). One study demonstrated that the removal of matrilin-3 from the chondrocyte pericellular matrix removes Indian hedgehog signaling, which is a staple mediator of mechanically regulating cartilage growth. The removal of matrilin-3 also mitigates mechanical stimulation of chondrocytes for proliferation and differentiation. On the other hand, increased expression of matrilin-3 also decreased the mechanical response of chondrocytes and indicates that the concentration of matrilin-3 play a role in stimulating cartilage growth (37). Matrilin-3 has also been shown to stimulate the chondrogenesis of progenitor cells and demonstrate the matrix protein have the ability to regulate cell behavior (38-40). Additionally, matrilin-3 possesses anti-inflammatory properties that ultimately inhibits chondrocyte hypertrophy through the BMP-2 pathway antagonist (41, 42). Biologically, Matrilin-3 antagonizes bone morphogenetic protein-2 (BMP-2) and VEGF to inhibit chondrocyte hypertrophy and suppress bone formation (42, 43). As a result of its properties, Matrilin-3 has potential to treat growth plate fractures to prevent bony bridge formation. However, the injection of Matrilin-3 in solution cannot ensure localization of its therapeutic effect at the injured site. Matrilin-3 has been found to have a greater bioactivity for cartilage homeostasis in a matrix

compared to solution form (44). This evidence suggests that it is critical to deliver Matrilin-3 as a matrix for our therapy.

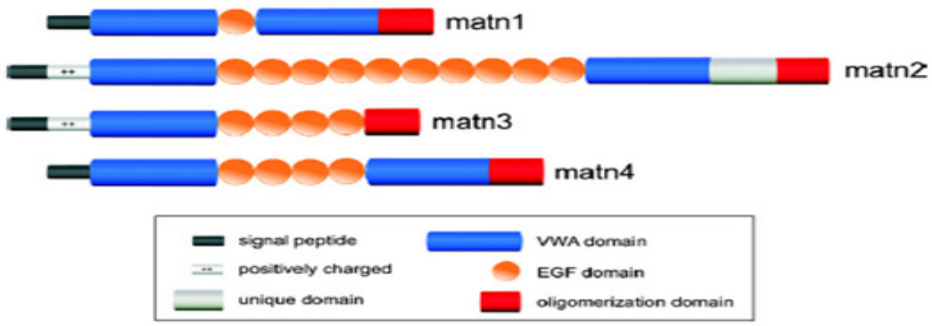

Figure. 4 Illustration of the structures of the protein in the matrilin family (34).

Rosette Nanotubes

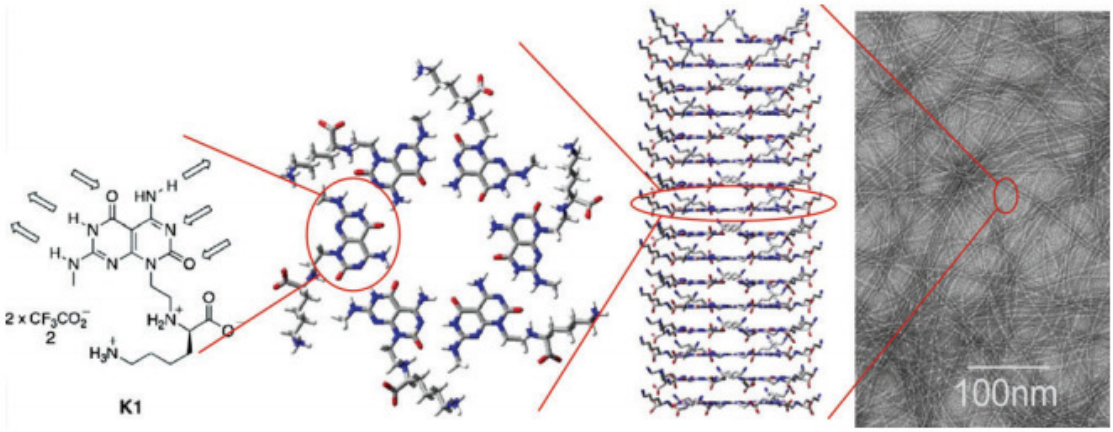

Figure 5. Illustration of the hierarchical formation process of rosette nanotubes (45).

Rosette nanotubes (RNTs) are a class of biomimetic self-assembled supramolecular structures. These nanotubes are made up of guanine and cytosine DNA base pairs with a side chain of lysine through linkage (45). In physiological conditions, these base pairs are able to self-assemble through a hierarchical process into a six-membered supermacrocycle held together by 18 hydrogen bonds as a result of electrostatic forces, hydrophobic effects, and base stacking interactions. The structure is then able to form a stable stack with a diameter of around 3.5 nanometers and an inner channel 11 A in diameter. The RNTs have been reported to have similar

characteristics compared to collagen in terms of size and morphology. They also have enhanced protein absorption and stem cell and chondrocyte functions (46). As a result of their properties, rosette nanotubes have been studied for their applications in tissue engineering and drug delivery. For example, one study conducted explored the drug loading capabilities of RNTs with cancer drugs. The findings indicate good loading of a hydrophobic drug, TAM, used in cancer therapy (47). Another study done demonstrated the use of RNTs along with a hydrogel to form a 3D scaffold for live cells. Results indicated the RNT structures were able to promote chondrogenic differentiation (46). Research has also shown increased cell adhesion and proliferation for various cell types including MSCs and chondrocytes (46, 48). Additionally, in vivo testing of the RNTs demonstrates great biocompatibility and low toxicity (49). The properties of the RNTs are desirable for our purpose to treat growth plate fractures.

Materials/Methods

Rosette Nanotube Synthesis

The rosette nanotubes used in the experiments were synthesized following techniques published in a paper by Fenniri et al. at Purdue University (50).

Nanomatrix Visualization

The mixture of RNT and MATN3 was lyophilized in a well plate to visualize the structure that the compound produces. The different groups used were nothing for control group, RNT alone, MATN3 alone, and the mixture of RNT and MATN3. The materials were mixed in deionized water in 1mL eppendorf tubes. For MATN3 alone, 2 µl of MATN3 at 500 µg/µl concentration was mixed with 300 µl of deionized water. 5 µl of RNT at 1g/L was added to another 300 µl of water for RNT alone. For the nanomatrix, 5 µl of RNT was first added to 300 µl of water. Afterwards, 2 µl of MATN3 was added to the solution. The RNT and MATN3 will

self assemble through the mixing of the two molecules from pipetting the solution up and down. The solutions for each group were left to rest for 5 minutes. For each group, 60 µl of solution was transferred into a 96 well plate into 5 wells for a total of 300 µl. All the steps were done under the hood for a sterile environment. The plate was then placed into the lyophilizer to freeze dry the plate at -80^{o}C to evaporate the water. Images of the wells were captured for each test group using a DSR camera. The RNT alone group and the nanomatrix were also imaged using transmission electron microscopy (TEM).

Cell Proliferation

A cell proliferation study was conducted using Human Umbilical Vein Cells (HUVEC) to see the effects of the nanomatrix on angiogenesis. This study consists of the control group with nothing, RNT alone, MATN3 alone and the nanomatrix of RNT plus MATN3. 10 µl of RNT was mixed in 300 µl of deionized water for the RNT alone group and 4 µl of MATN3 was added to 300 µl of deionized water for the MATN3 alone group. The same amounts of each component was used for the nanomatrix test group. The concentrations of the components used are the same throughout the thesis. The study was conducted using an 8 well plate. 150 µl of solution was added to 2 wells for each group. 150 µl of deionized water was added to two wells for the control group. The plate was then lyophilized at -80oC to evaporate the water. Afterwards, 10,000 HUVEC cells were seeded into each well. HUVEC cell media was then added to each well. Finally, the plate was incubated to let the cells proliferate. Cell media was changed every 2 days. After 6 days, the cells in each well were prepared for quantification using the CyQUANT Cell Proliferation Assay from Thermofisher. Cell media was aspirated out of each well carefully. The plate was then frozen at -70^{o}C overnight. 4.75 mL of deionized water was mixed with 250 µl of

cell lysis buffer and 12.5 µl of CyQUANT GR dye in a 15 mL tube. Aluminum foil was wrapped around the tube to protect the dye from photobleaching. Once ready, the plate was thawed at room temperature and 400 µl of the mixture was added to each well in the plate and left to sit in for 10 minutes with protection from light. Each well was then transferred into a 96 well plate, with 200 µl per well. The plate was then analyzed using a MDC SpectraMax Gemini EM Microplate Reader to quantify the number of cells in each well for the different test groups.

Fluorescence Labeling of RNT and MATN3

The RNT and MATN3 were labeled with a fluorescence dye to track its presence *in vivo*. The MATN3 were dyed with AlexaFluor 680 and RNT with AlexaFluor 750. The 2 molecules were dyed with different wavelengths because it will be used to track the clearance of the nanomatrix. The MATN3 will be tracked using 680 nm wavelength and 750 nm wavelength for RNT. After the molecules were dyed, the solution was purified using HPLC to remove any excess dye that did not mix with the proteins as well as other byproducts.

Nanomatrix preparation for in vivo Study

For the *in vivo* study, RNT alone, MATN alone, and the RNT/MATN3 nanomatrix was tested. The solutions before injection was prepared similar to previous experiments, using the same amount of each molecule. However, the solutions were mixed in 10% agarose solution made in HBS media instead of deionized water. The agarose solutions were kept in a heating block at 32^{o}C to prevent the mixture from gelling until the injection.

In vivo injection of RNT/MATN3 nanomatrix

5 week old rats were prepared prior to the injection of the nanomatrix for the clearance study following the approved IACUC protocol. A total of 3 rats were used for the study, one for each test group. Each rat was sedated temporarily using a vacuum chamber, where the rat was subjected to inhalation of isoflurane. Once unconscious, 300 µl of ketamine was injected into the lower left abdomen with a syringe. The sedated rats were left for 5 minutes for the ketamine to kick in. Afterwards, the bottom half of the rats were shaved to expose the knee and to prevent any noise in the fluorescence molecular tomography (FMT) imaging. Prior to injection of the nanomatrix, each rat was imaged using FMT to get a baseline. Each rat was imaged using the 680 nm and 750 nm channel. A drill hole was made in the proximal tibia through a cortical window and was continued through the medial side of the growth plate. Afterwards, the agarose solutions were injected into the left and right knee joint of each rat for each test group. The injected rats were then imaged again using FMT to get the intensity levels at each knee joint at 680nm and 750 nm. After imaging, the rats were placed back into their cage with access to water and food.

Fluorescence molecular tomography of rats

The rats were monitored daily for one week to get data at different time points. Each day, the rats were sedated with isoflurane temporarily, followed by an injection of 300 µl of ketamine into the lower right abdomen of the rat. Once the rat was fully sedated, they were placed onto the FMT cassette for imaging. The limbs were secured with tape to fit both knee joints into the same imaging window on the FMT. Each knee joint was imaged using the 680 nm and 750 nm channel

for RNT and MATN3. Afterwards, rats were placed back into their cage with access to food and water.

Therapeutic assessment of MATN3/RNT nanomatrix in vivo

5 week old rats were prepared prior to the injection of the nanomatrix for the efficacy study following the approved IACUC protocol. Each rat was sedated temporarily using a vacuum chamber, where the rat was subjected to inhalation of isoflurane. Once unconscious, 300 µl of ketamine was injected into the lower left abdomen with a syringe. The sedated rats were left for 5 minutes for the ketamine to kick in. Afterwards, the bottom half of the rats were shaved to expose the knee. The nanomatrix was prepared following previous protocol used for *in vivo* study. The right tibia of the rats were imaged using Faxitron X-ray before surgery. A control group with no treatment and three treatment groups using the nanomatrix, MATN3 alone and RNT alone was used for this study, with one rat per group. A drill hole was made in the right proximal tibia through a cortical window and was continued through the medial side of the growth plate. The nanomatrix was then injected into the injury site. Afterwards, the rats were placed back into their cage with access to food and water. The test subjects were imaged using X-ray 4, 6, 8, 10, and 12 weeks after surgery. At week 12 the subjects were euthanized. The X-ray images were used to assess the degree of bone deformity.

Nanomatrix loaded with growth factors

The nanomatrix was prepared for a chondrogenesis study. This study consisted of 5 test groups. The negative control was nothing added to the cells. The positive control was adding growth factors each time the media was changed. 10 µg of TGF-B1 and 100 µg of IGF-1 was added each time. The next group was the nanomatrix. 8ul of MATN3 at 500 µg/µl and 20 µl of

RNT was mixed in 1.2 mL of deionized water. The last test group consisted of adding growth factors to the nanomatrix. 2 µl of TGF-B1 at 100 ng/µl and 2uL of IGF-1 at 1 µg/µl was mixed in 200 µL of deionized water. Then 2.5 µl of 1mM Ca2+ was added to the mixture. 8 µl of MATN3 was then added to the growth factors. The solution was left for 10 minutes to bind the growth factors. Afterwards, 20 µl of RNT was mixed into the solution and left for 5 minutes. Finally, the solution was diluted with 1mL of deionized water.

Chondrogenesis study

The chondrogenesis study was done using a 24 well plate. 300 µl of nanomatrix solution was added to 4 wells for each test group. For the positive and negative controls, 300 µl of deionized water was added to 8 wells in total. 2 plates were prepared to analyze the results at 2 different time points. This means that the amounts mixed in the nanomatrix mentioned above is only for 1 plate. The 2 plates were lyophilized at -80^{o}C to evaporate the water. After the plates have been lyophilized, cells from the ATDC5 chondrogenic cell line was seeded into the wells. 100,000 ATDC5 cells were seeded into each well, for a total of 16 wells for each plate. The growth factors were added to the wells for the positive control group. The plates were then placed inside the incubator. The cell media was changed every 2-3 days. The plates were analyzed using qPCR at 7 day and 14 day time points. The samples for each test group was prepared following the RNA isolation protocol from Thermofisher. The samples were then analyzed using qPCR for Col2a1 and ACAN cell markers for evidence of differentiation into chondrocytes.

Results

Self-assembly of nanomatrix

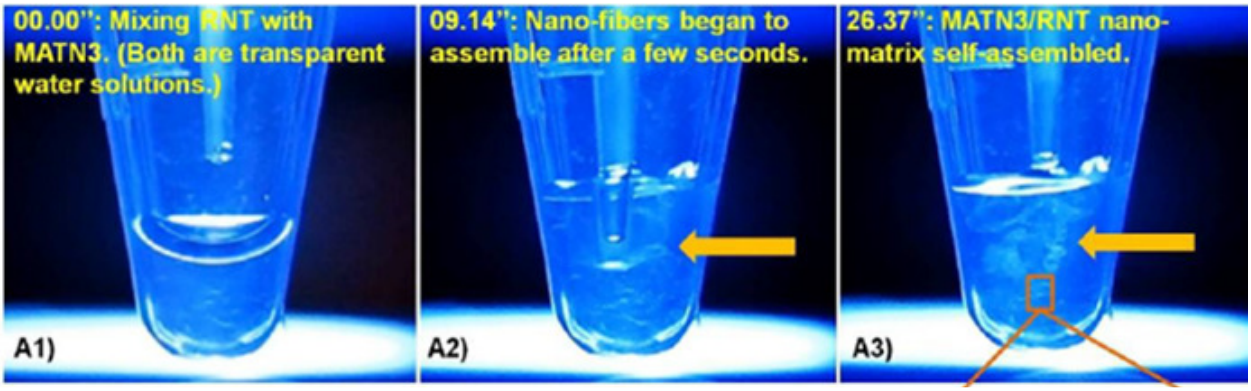

Figure 6. Images of the RNT and MATN3 self-assembling in solution over the span of 30 seconds.

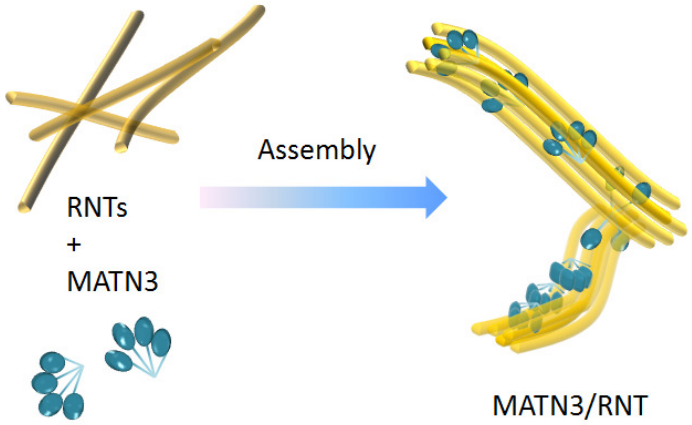

Figure 7. Illustration of the assembly of MATN3/RNT nanomatrix

The RNT and MATN3 were observed to self-assemble in solution. Figure 6 shows screen shots of a video showing the self-assembly of the nanomatrix in solution. In the video, the two materials were mixed in solution using a pipette. After 10 seconds, there was visible formation of the matrix in the solution and continued to form in the video for approximately 30 seconds. An illustration of the assembly can be seen in Figure 7. The two materials are able to self assemble due to electrostatic attraction between the negatively charged MATN3 and the positively charged RNTs. In addition, RNTs biomimics the structure of collagen and MATN3 have been found to

naturally bind to collagen-like structures (51). The ability to self-assemble in solution by the RNTs and MATN3 is desirable for our treatment, since the materials can be injected in solution into the fracture site and assemble into the nanomatrix. The growth plate is inside the bone and makes the implantation of pre-assembled matrices difficult and require intensive surgery.

Nanomatrix structure

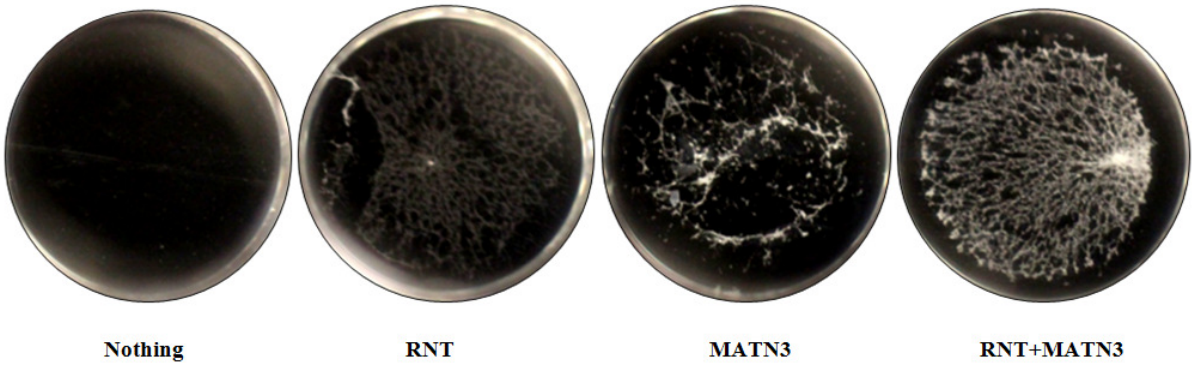

Figure 8. Images of the lyophilized nanomatrix

The images of the lyophilized well plates can be seen in Figure 8. The results show good structures forming on the well plate for the RNT group and the RNT+MATN3 nanomatrix group. For MATN3 alone, there is minimal structure that is formed and does not cover the entire well. The nanomatrix seem to have a more complete coverage of the well compared to the RNT alone group. These results demonstrate that the self assembly of RNT and MATN3 is able to form 3-D structures to provide a scaffold for cells. The TEM images taken can be seen in Figure 9. The image of RNT alone shows bundle like structure of the RNTs. When the MATN3 was mixed with the RNTs to form the nanomatrix, the bundles were enlarged compared to RNT alone. The final image on the right shows the nanomatrix at a higher magnification. The image shows white spots within the RNT bundle and suggests that the MATN3 is imbedded within the RNTs.

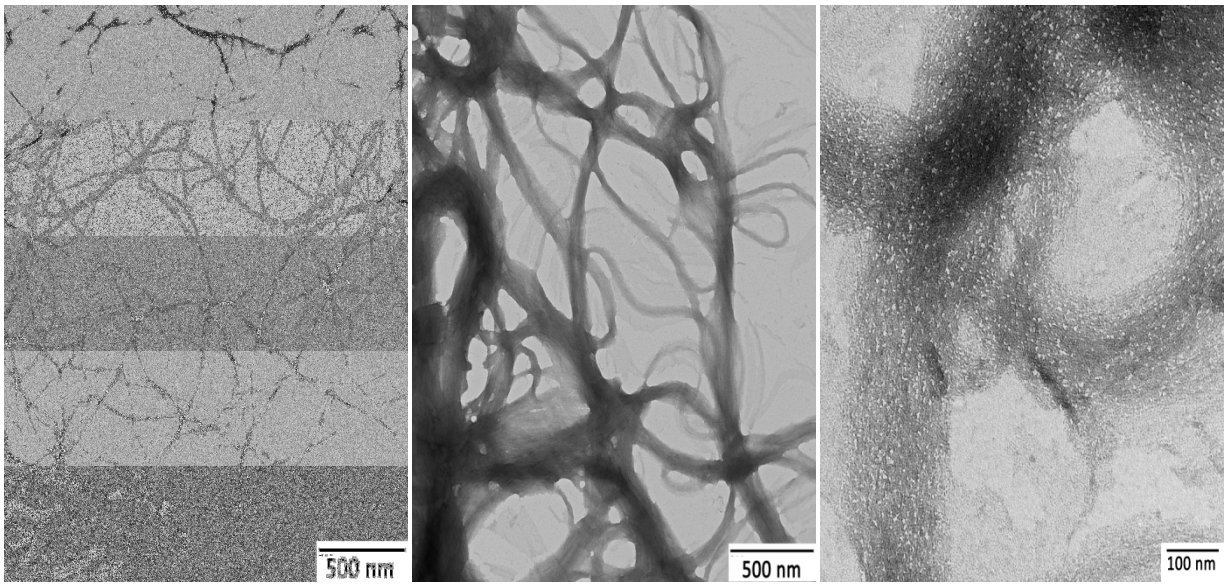

Figure 9. TEM images of the RNT only (left) and RNT/MATN3 nanomatrix (center and right). The image on the right of the nanomatrix is at a higher magnification

Proliferation of HUVEC

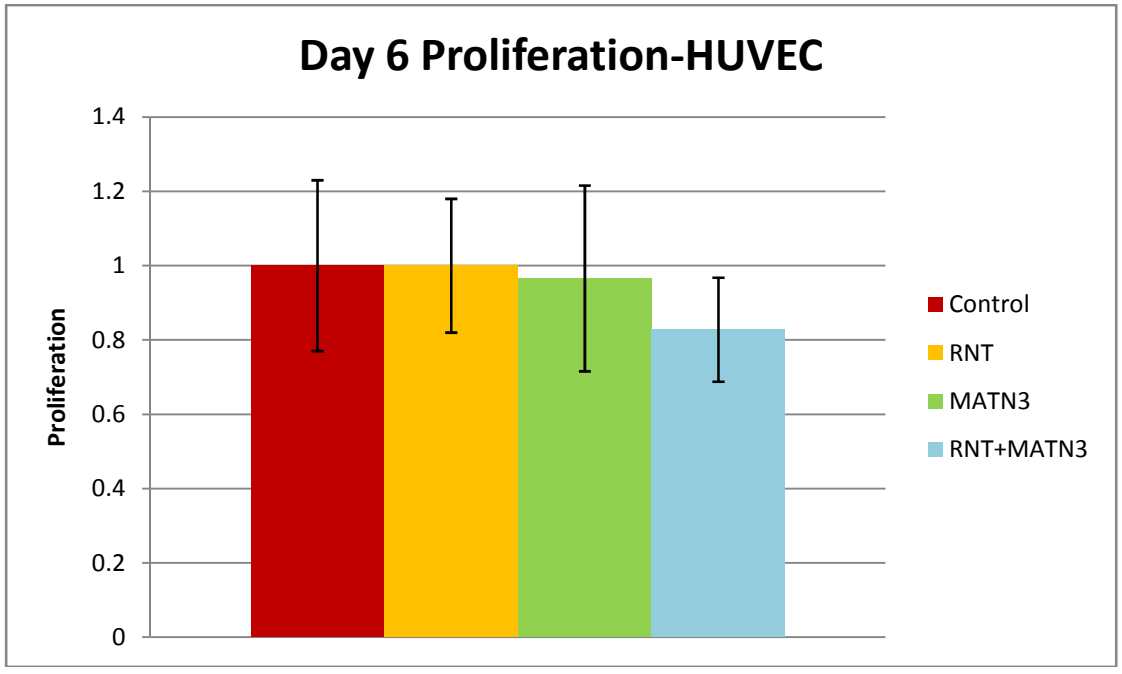

Figure 10. The proliferation of HUVEC cells for the RNT alone, MATN3 alone, and RNT/MATN3 nanomatrix test groups. The data was normalized against the control group.

The cell proliferation results for HUVEC cells can be seen in Figure 10. The results show similar cell proliferation from the RNT alone and MATN3 alone group compared to the control

group. The RNT+MATN3 group show a decrease to around 80 percent proliferation but with no statistical significance. This results suggests that the combination of RNT and MATN3 has the potential to hinder angiogenesis, which is a desired property for the treatment of growth plate fractures to prevent bony bridge formation.

Retention of MATN3 in vivo

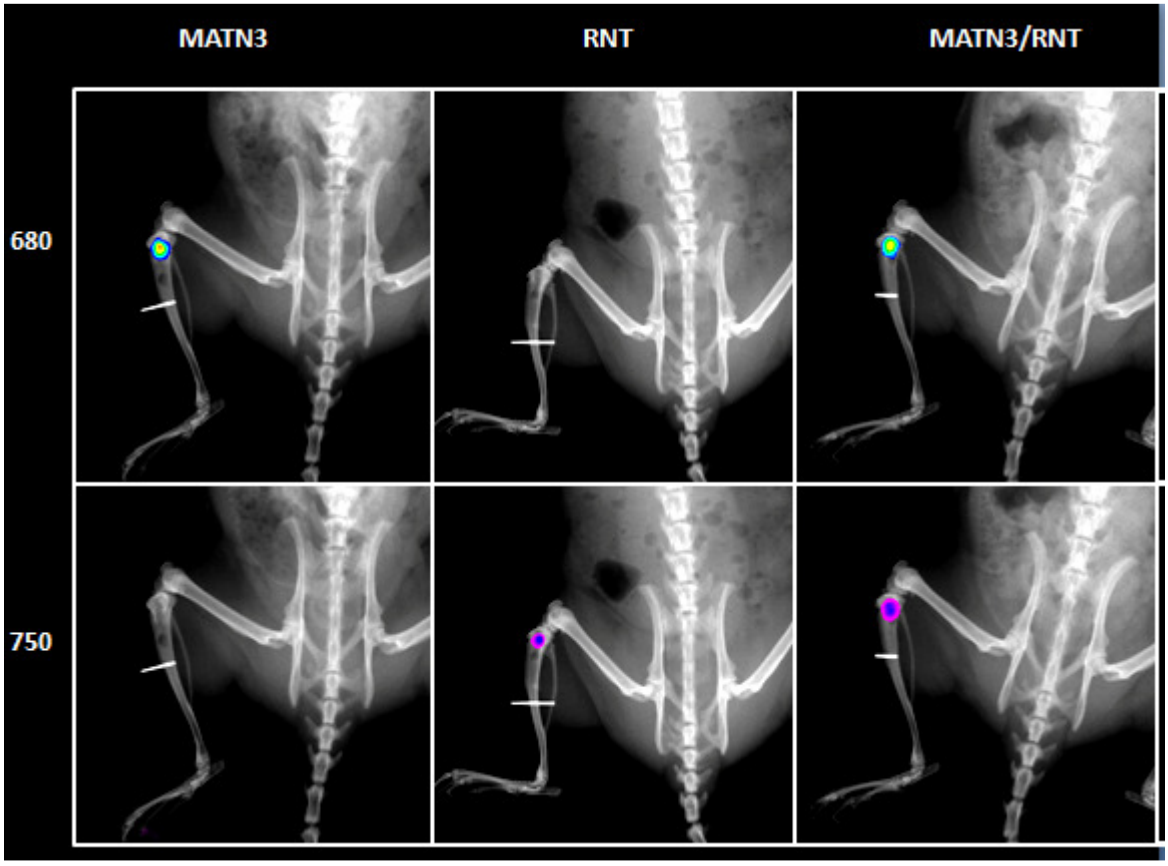

Figure 11. FMT images of knee joint showing fluorescence signal at 680 nm and 750 nm for MATN3 alone, RNT alone, and the nanomatrix of RNT and MATN3.

The figure above shows FMT images of the rats right after the injection of the nanomatrix. For MATN3, the figure shows a fluorescence signal at 680 nm and no signal at 750 nm. The RNT images shows a signal at 750 nm and not at 680 nm. Finally, the images for the nanomatrix of RNT and MATN3 shows signals at both the 680 nm and 750 nm channels. The

results shows that the labeling of the MATN3 and RNT was successful and it is capable of being detected by FMT. The fluorescence signals for 7 days were plotted in Figure 12 and the data was normalized against the fluorescence signal. From the results, the MATN3 alone and RNT alone test groups were basically completely cleared out after day 7. However, for the RNT in the nanomatrix, there were still around 10% of the signal left from the nanomatrix. For the MATN3 in the nanomatrix, there is around 40% of the signal left after day 7. The results indicate that the MATN3 delivered in the nanomatrix with RNT was able to retain approximately 10 times more compared to delivering MATN3 alone at the fracture site.

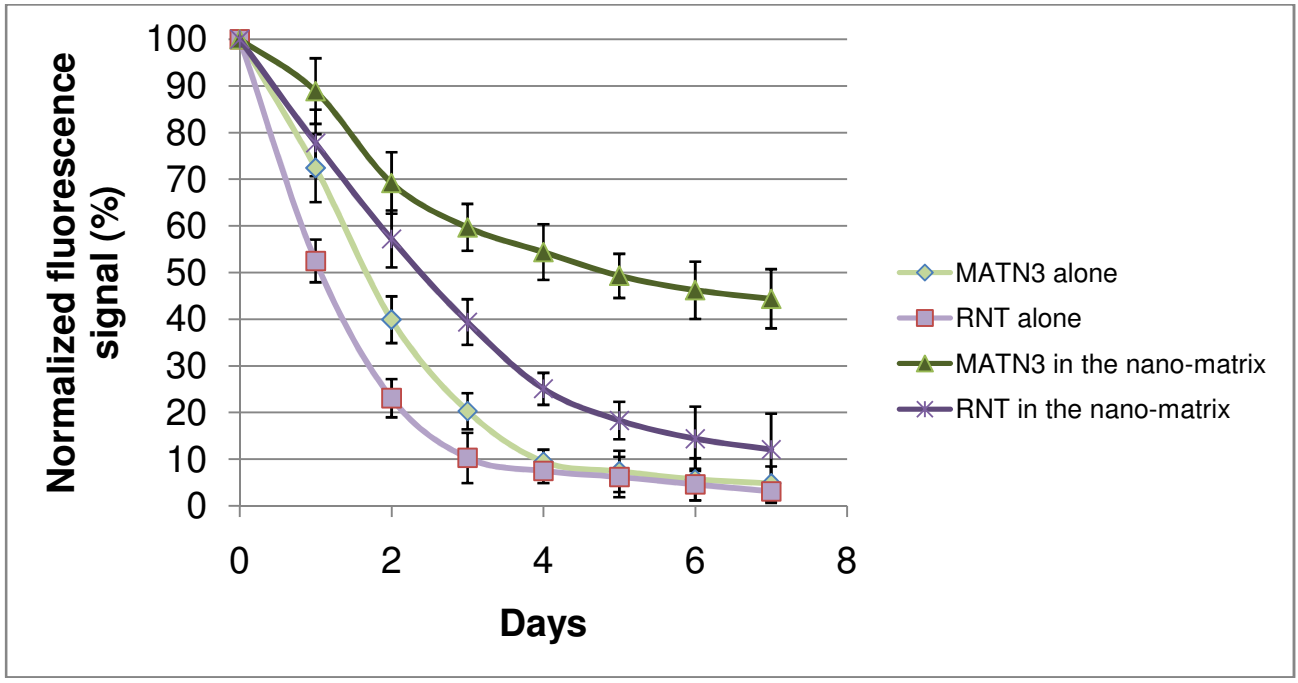

Figure 12. Graph of the fluorescence signal of the 3 test groups over the period of 7 days.

Therapeutic Effect of Nanomatrix

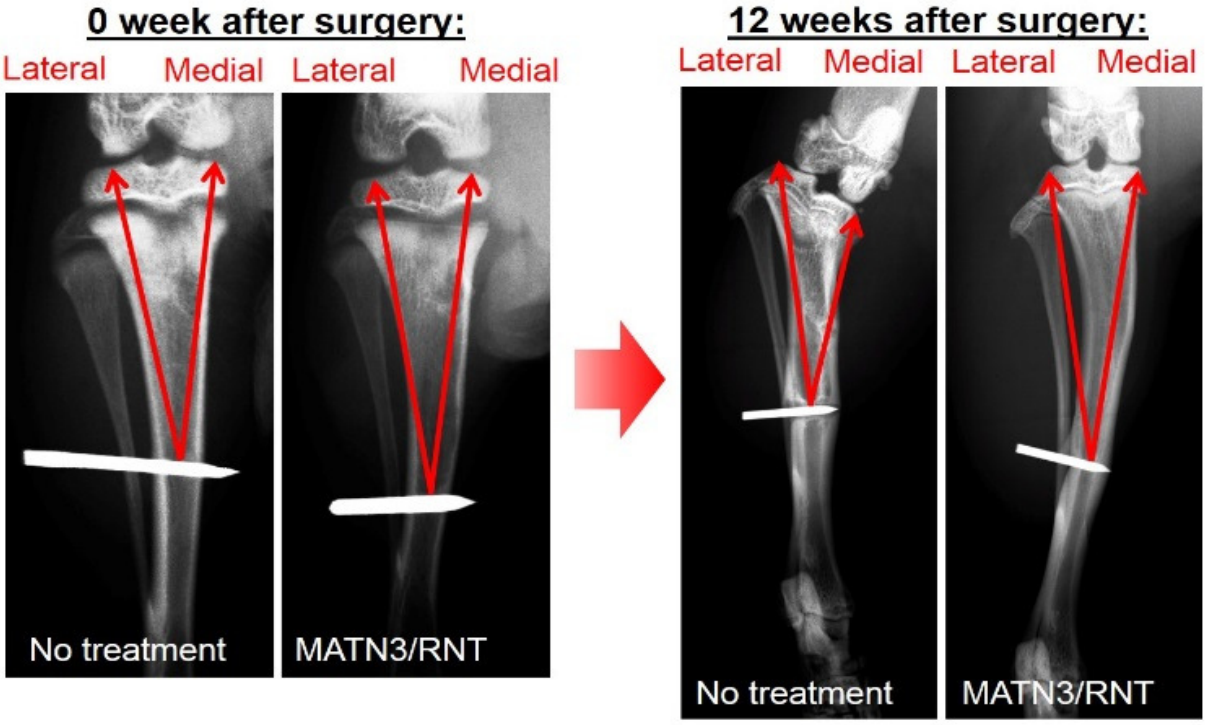

Figure 13. X-ray images of the rat tibia before surgery and 12 weeks post-surgery showing no treatment group (control) and the treatment group using the MATN3/RNT nanomatrix.

The X-ray images of the tibia for before surgery and 12 week post surgery can be seen in Figure 13. The degree of bone deformity and modulation of growth with the experimental nanomatrix was assessed base on the distance from the transverse k-wire in the middle of the tibia. The results show a significant deformity for the no treatment group based on the images prior to surgery and 12 weeks post surgery. The distance from the middle of the tibia at the k-wire is different between the lateral and medial side, illustrated by the red arrows in the image. This demonstrates the effect of a growth plate injury in causing bone deformity. However, the results for the treatment group with the MATN3/RNT nanomatrix were different. Comparing the pre-surgery and post surgery images, the results indicate little differences between the two. Moreover, the distance from the middle of the bone to the lateral and medial side were relatively

the same, which suggests that the nanomatrix was able to improve the healing of the growth plate after fracture. Although not shown in the results, the outcome of the MATN3 alone and RNT alone test groups had a slight reduction in the deformity but not as significant as using the nanomatrix of MATN3 and RNT.

Chondrogenesis Using Growth Factors

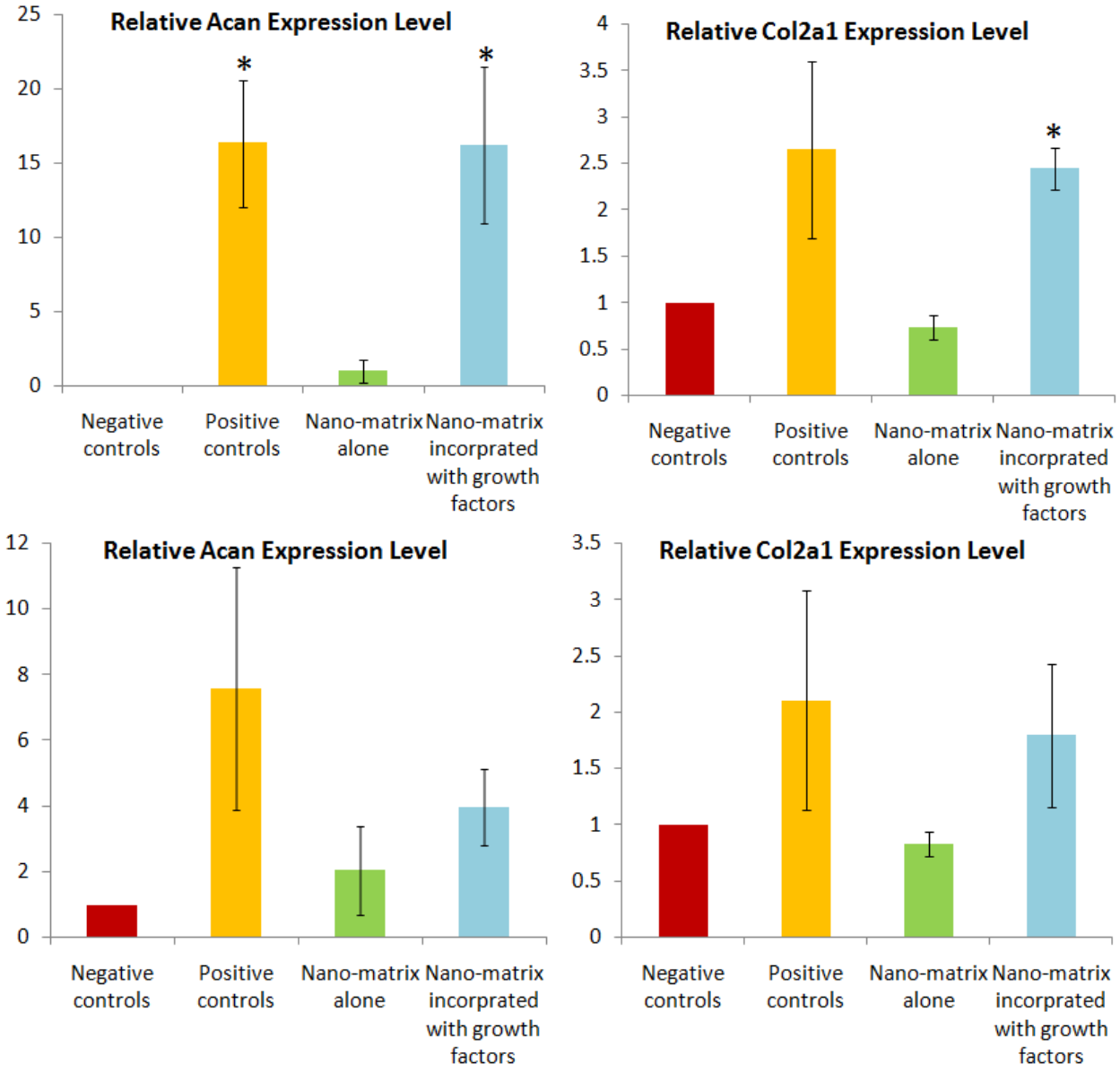

Figure 14. Expression level of Col2a1 and ACAN cells markers at day 7 (top) and day 14 (bottom) for the chondrogenesis study. There is statistical significance at $p<0.05$ at day 7 when compared to negative control or nanomatrix alone.

The results for the chondrogenesis study can be seen in Figure 14. At day 7, the results show a significant difference in expression of ACAN and Col2a1 for the positive control group and nanomatrix with growth factors compared to the negative control and nanomatrix alone. The expression levels were similar between the positive control group and nanomatrix with growth factors for both markers. It is interesting to note this trend because the positive control group consisted of adding growth factors each time the cell media was changed. At day 7, the cell media was changed twice, which means the dosing of the growth factors were 3 times higher compared to the growth factors in the nanomatrix. Since the expression levels were similar, the results suggests that the nanomatrix was able to sustain the effect the growth factors at a lower dose compared to the positive control. At day 14, the results show higher expression levels in the positive control and nanomatrix with growth factors compared to the other two groups with no significant difference. The expression levels were lower for the nanomatrix with growth factors compared to the positive control and not as close compared to the results for day 7. This could suggest a decay in the effect of the growth factors in the nanomatrix after day 7.

Discussion/Conclusion

Growth plate fractures pose a significant problem for children affected by it. Minor injuries to the growth plate have a high success in recovering without any complications in bone growth or cause any deformity. However, the more serious fractures that are mainly classified as type III and type IV fractures have poor prognosis in healing properly and have a high chance of causing bone deformity or uneven bone growth due to the bony bridge formation in the growth plate. Currently there is no biological therapy that is able to prevent the bony bridge formation in

the growth plate and require anyone affected by it to obtain surgery to remove the bony bridge or to correct any uneven bone growth.

This study examines the use of a novel therapy using rosette nanotubes and matrilin-3 that are able to self-assemble into a nanomatrix to reduce the bony bridge formation in fractured growth plates. In the beginning, we observed the self-assembly of the MATN3 and RNT in solution in a short amount of time in solution due to electrostatic interaction and the tendency of MATN3 to bind to collagen like structures. The structure of the matrix was analyzed at the macro and nanoscale. The results show good formation of 3-D structure by the nanomatrix to provide a scaffold for recruited cells in the growth plate. Images taken using TEM of the nanomatrix indicate the MATN3 was embedded into the RNTs. The *in vitro* study done using HUVEC cells demonstrated potential inhibition of the growth of blood vessels by the nanomatrix. Since bony bridge formation is linked to angiogenesis, the nanomatrix's ability to inhibit angiogenesis is desirable to make the therapy effective. The *in vivo* experiment using rats demonstrated that the injection of the nanomatrix in the growth plate fracture site allowed the MATN3 to remain in the body much longer compared to injection of just MATN3 alone. The increased retention time of MATN3 from the nanomatrix is desired to maximize its effect on promoting chondrogenesis and inhibiting angiogenesis in the growth plate since delivering the protein in solution form is not as effective. More importantly, the nanomatrix was able to improve the healing of the growth plate from the assessment using the growth plate fracture animal model. There was a significant deformity in the no treatment group compared to the group that received the treatment of MATN3/RNT nanomatrix. The nanomatrix of RNT and MATN3 for treatment of growth plate fractures show promising results. Although the results indicate improvement in the treatment of the growth plate fracture, the healing is not 100%

perfect and further research can be done to increase its efficacy. A preliminary study was done that assessed the efficacy of the nanomatrix incorporated with the IGF-1 and TGF-B1 growth factors in promoting chondrogenesis. The results suggests the nanomatrix is able to promote chondrogenesis with the growth factors with the about the same effectiveness as delivering growth factors alone at a much lower dosage.

Future studies needs to be done to validate the therapy further. More animal studies can be done to validate its effectiveness in preventing the bony bridge formation by increasing the sample size. The incorporation of growth factors in the nanomatrix should also be tested *in vivo* to determine whether or not the efficacy of the treatment is increased. The time between when the fracture occurs and when the treatment is administered can also be explored to determine the effect it might have on the efficacy of the treatment, since patients who require treatment for growth plate fractures will not receive it immediately.

References

1. Gross Anatomy. *Boundless Anatomy and Physiology Boundless*, October 2016. Retrieved April 12, 2017, from https://www.boundless.com/physiology/textbooks/boundless-anatomy-and-physiology-textbook/skeletal-system-6/introduction-to-bone-71/gross-anatomy-435-1161/

2. Dayton, P., Feilmeier, M., & Coleman, N. (2013). Principles of management of growth plate fractures in the foot and ankle. *Clinics in Podiatric Medicine and Surgery, 30*(4), 583-598.

3. Burdan, F., Szumiło, J., Korobowicz, A., Farooquee, R., Patel, S., Patel, A., . . . Dudka, J. (2009). Morphology and physiology of the epiphyseal growth plate. *Folia Histochemica Et Cytobiologica*, 47(1), 5-16.

4. Panagis, J., Ballock, T., Ehrlich, M., Goodwin, R., & Salter, R. (2014). Questions and Answers about Growth Plate Injuries. Retrieved December 20, 2016, from https://www.niams.nih.gov/health_info/growth_plate_injuries/

5. Chung, R., & Xian, C. J. (2014). Recent research on the growth plate: Mechanisms for growth plate injury repair and potential cell-based therapies for regeneration. *Journal of Molecular Endocrinology*, 53(1), T45-T61.

6. Zhou, F. H., Foster, B. K., Sander, G., & Xian, C. J. (2004). Expression of proinflammatory cytokines and growth factors at the injured growth plate cartilage in young rats. *Bone*, 35(6), 1307-1315.

7. Chung, R., Cool, J.C., Scherer, M.A., Foster, B.K. & Xian, C.J. (2006). Roles of neutrophil-mediated inflammatory response in the bony repair of injured growth plate cartilage in young rats. *Journal of Leukocyte Biology* 80(6), 1272–1280.

8. Xian, C. J., Zhou, F. H., McCarty, R. C., & Foster, B. K. (2004). Intramembranous ossification mechanism for bone bridge formation at the growth plate cartilage injury site. *Journal of Orthopaedic Research*, 22(2), 417-426.

9. Jaramillo, D., Shapiro, F., Hoffer, F. A., Winalski, C. S., Koskinen, M. F., Frasso, R., & Johnson, A. (1990). Posttraumatic growth-plate abnormalities: MR imaging of bony-bridge formation in rabbits. *Radiology*, 175(3), 767-773.

10. Schindeler, A., McDonald, M. M., Bokko, P., & Little, D. G. (2008). Bone remodeling during fracture repair: The cellular picture. *Seminars in Cell and Developmental Biology*, 19(5), 459-466.

11. Minguell, J. J., Erices, A., & Conget, P. (2001). Mesenchymal stem cells. *Experimental Biology and Medicine*, 226(6), 507.

12. Ngo, T. Q., Scherer, M. A., Zhou, F. H., Foster, B. K., & Xian, C. J. (2006). Expression of bone morphogenic proteins and receptors at the injured growth plate cartilage in young rats. *Journal of Histochemistry and Cytochemistry*, 54(8), 945-954.

13. Arasapam, G., Scherer, M., Cool, J. C., Foster, B. K., & Xian, C. J. (2006). Roles of COX-2 and iNOS in the bony repair of the injured growth plate cartilage. *Journal of Cellular Biochemistry*, 99(2), 450-461.

14. Fischerauer, E., Heidari, N., Neumayer, B., Deutsch, A., & Weinberg, A. M. (2011). The spatial and temporal expression of VEGF and its receptors 1 and 2 in post-traumatic bone bridge formation of the growth plate. *Journal of Molecular Histology*, 42(6), 513-522.

15. Yang, Y. Q., Tan Y.Y, Wong, R., Wenden, A., Zhang, L.K., Rabie, A. B. (2012). The role of vascular endothelial growth factor in ossification. *Journal of Oral Science*, 4(2), 64-68.

16. Fischerauer, E. E., Manninger, M., Seles, M., Janezic, G., Pichler, K., Ebner, B., & Weinberg, A. M. (2013). BMP-6 and BMPR-1a are up-regulated in the growth plate of the fractured tibia. *Journal of Orthopaedic Research,* 31(3), 357-363.

17. Macsai, C. E., Hopwood, B., Chung, R., Foster, B. K., & Xian, C. J. (2011). Structural and molecular analyses of bone bridge formation within the growth plate injury site and cartilage degeneration at the adjacent uninjured area. *Bone*, 49(4), 904-912.

18. Musumeci, G., Castrogiovanni, P., Loreto, C., Castorina, S., Pichler, K., & Weinberg, A. M. (2013). Post-traumatic caspase-3 expression in the adjacent areas of growth plate injury site: A morphological study. *International Journal of Molecular Sciences*, 14(8), 15767-15784.

19. Ortega, N., Behonick, D. J., & Werb, Z. (2004). Matrix remodeling during endochondral ossification. *Trends in Cell Biology*, 14(2), 86-93.

20. Brandi, M. L., & Collin-Osdoby, P. (2006). Vascular biology and the skeleton. *Journal of Bone and Mineral Research*, 21(2), 183-192.

21. Chim, S. M., Tickner, J., Chow, S. T., Kuek, V., Guo, B., Zhang, G., . . . Xu, J. (2013). Angiogenic factors in bone local environment. *Cytokine and Growth Factor Reviews*, 24(3), 297.

22. Chung, R., Foster, B. K., Zannettino, A. C. W., & Xian, C. J. (2009). Potential roles of growth factor PDGF-BB in the bony repair of injured growth plate. *Bone*, 44(5), 878-885.

23. Baumgart, R. (2009). The reverse planning method for lengthening of the lower limb using a straight intramedullary nail with or without deformity correction. A new method. *Operative Orthopädie Und Traumatologie*, 21(2), 221-233.

24. Langenskiold, A. (1981). Surgical treatment of partial closure of the growth plate. *Journal of Pediatric Orthopedics*, 1, 3-11.

25. Tobita, M., Ochi, M., Uchio, Y., Mori, R., Iwasa, J., Katsube, K., & Motomura, T. (2002). Treatment of growth plate injury with autogenous chondrocytes: A study in rabbits. *Acta Orthopaedica Scandinavica*, 73(3), 352.

26. Toolan, B. C., Frenkel, S. R., Pereira, D. S., & Alexander, H. (1998). Development of a novel osteochondral graft for cartilage repair. *Journal of Biomedical Materials Research*, 41(2), 244-250.

27. Li, W., Xu, R., Xue, Y., Huang, J., & Gao, Y. (2013). Treatment of growth plate injury with microencapsulated chondrocytes. *Biotechnology and Bioprocess Engineering*, 18(4), 655-662.

28. Chen, F., Hui, J. H. P., Chan, W. K., & Lee, E. H. (2003). Cultured mesenchymal stem cell transfers in the treatment of partial growth arrest. *Journal of Pediatric Orthopaedics*, 23(4), 425-429.

29. McCarty, R. C., Xian, C. J., Gronthos, S., Zannettino, A. C. W., & Foster, B. K. (2010). Application of autologous bone marrow derived mesenchymal stem cells to an ovine model of growth plate cartilage injury. *The Open Orthopaedics Journal*, 4, 204.

30. McCarty, R. C., Gronthos, S., Zannettino, A. C., Foster, B. K., & Xian, C. J. (2009). Characterisation and developmental potential of ovine bone marrow derived mesenchymal stem cells. *Journal of Cellular Physiology*, 219(2), 324-333.

31. Fukumoto, T., Sperling, J. W., Sanyal, A., Fitzsimmons, J. S., Reinholz, G. G., Conover, C. A., & O'Driscoll, S. W. (2003). Combined effects of insulin-like growth factor-1 and transforming growth factor-beta1 on periosteal mesenchymal cells during chondrogenesis in vitro. *Osteoarthritis and Cartilage / OARS, Osteoarthritis Research Society*, 11(1), 55.

32. Hutmacher, D. W. (2000). Scaffolds in tissue engineering bone and cartilage. *Biomaterials*, 21(24), 2529-2543.

33. Drury, J. L., & Mooney, D. J. (2003). Hydrogels for tissue engineering: Scaffold design variables and applications. *Biomaterials*, 24, 4337–4351.

34. Klatt, A. R., Becker, A. A., Neacsu, C. D., Paulsson, M., & Wagener, R. (2011). The matrilins: Modulators of extracellular matrix assembly. *International Journal of Biochemistry and Cell Biology*, 43(3), 320-330.

35. Klatt, A. R., Nitsche, D. P., Kobbe, B., MÃ¶rgelin, M., Paulsson, M., Wagener, R., . . . Lund University. (2000). Molecular structure and tissue distribution of matrilin-3, a filament-forming extracellular matrix protein expressed during skeletal development. *Journal of Biological Chemistry*, 275(6), 3999-4006.

36. Klatt, A. R., Paulsson, M., & Wagener, R. (2002). Expression of matrilins during maturation of mouse skeletal tissues. *Matrix Biology*, 21(3), 289-296.

37. Kanbe, K., Yang, X., Wei, L., Sun, C., & Chen, Q. (2007). Pericellular matrilins regulate activation of chondrocytes by cyclic Load-Induced matrix deformation. *Journal of Bone and Mineral Research*, 22(2), 318-328.

38. Jayasuriya, C. T., Chen, Y., Liu, W., & Chen, Q. (2016). The influence of tissue microenvironment on stem cell–based cartilage repair. *Annals of the New York Academy of Sciences*, 1383(1), 21-33.

39. Pei, M., Luo, J., & Chen, Q. (2008). Enhancing and maintaining chondrogenesis of synovial fibroblasts by cartilage extracellular matrix protein matrilins. *Osteoarthritis and Cartilage*, 16(9), 1110-1117.

40. Jayasuriya, C. T., Zhou, F. H., Pei, M., Wang, Z., Lemme, N. J., Haines, P., & Chen, Q. (2014). Matrilin-3 chondrodysplasia mutations cause attenuated chondrogenesis, premature hypertrophy and aberrant response to TGF-β in chondroprogenitor cells. *International Journal of Molecular Sciences*, 15(8), 14555-14573.

41. Jayasuriya, C. T., Goldring, M. B., Terek, R., & Chen, Q. (2012). Matrilin-3 induction of IL-1 receptor antagonist is required for up-regulating collagen II and aggrecan and down-regulating ADAMTS-5 gene expression. *Arthritis Research & Therapy*, 14(5), R197-R197.

42. Yang, X., Trehan, S. K., Guan, Y., Sun, C., Moore, D. C., Jayasuriya, C. T., & Chen, Q. (2014). Matrilin-3 inhibits chondrocyte hypertrophy as a bone morphogenetic protein-2 antagonist. *The Journal of Biological Chemistry*, 289(50), 34768-34779.

43. van der Weyden, L., Wei, L., Luo, J., Yang, X., Birk, D. E., Adams, D. J., &Chen, Q. (2006). Functional knockout of the matrilin-3 gene causes premature chondrocyte maturation to hypertrophy and increases bone mineral density and osteoarthritis. *The American Journal of Pathology*, 169(2), 515-527.

44. Vincourt, J., Etienne, S., Grossin, L., Cottet, J., Bantsimba-Malanda, C., Netter, P., . . . Magdalou, J. (2012). Matrilin-3 switches from anti- to pro-anabolic upon integration to the extracellular matrix. *Matrix Biology : Journal of the International Society for Matrix Biology*, 31(5), 290.

45. Zhang, L., Chen, Y., Rodriguez, J., Fenniri, H., & Webster, T. J. (2008). Biomimetic helical rosette nanotubes and nanocrystalline hydroxyapatite coatings on titanium for improving orthopedic implants. *International Journal of Nanomedicine*, 3(3), 323-334.

46. Chen, Y., Bilgen, B., Pareta, R. A., Myles, A. J., Fenniri, H., Ciombor, D. M., . . . Webster, T. J. (2010). Self-assembled rosette nanotube/hydrogel composites for cartilage tissue engineering. Tissue Engineering. Part C, Methods, 16(6), 1233-1243.

47. Song, S., Chen, Y., Yan, Z., Fenniri, H., & Webster, T. J. (2011). Self-assembled rosette nanotubes for incorporating hydrophobic drugs in physiological environments. *International Journal of Nanomedicine*, 6, 101-107.

48. Fine, E., Zhang, L., Fenniri, H., & Webster, T. J. (2009). Enhanced endothelial cell functions on rosette nanotube-coated titanium vascular stents. *International Journal of Nanomedicine*, 4, 91-97.

49. Journeay, W. S., Suri, S. S., Moralez, J. G., Fenniri, H., & Singh, B. (2008). Rosette nanotubes show low acute pulmonary toxicity in vivo. *International Journal of Nanomedicine*, 2008, 373-383.

50. Fenniri, H., Deng, B., & Ribbe, A. E. (2002). Helical rosette nanotubes with tunable chiroptical properties. *Journal of the American Chemical Society, 124*(37), 11064-11072.

51. Winterbottom, N., Tondravi, M. M., Harrington, T. L., Klier, F. G., Vertel, B. M., & Goetinck, P. F. (1992). Cartilage matrix protein is a component of the collagen fibril of cartilage. *Developmental Dynamics : An Official Publication of the American Association of Anatomists*, 193(3), 266-276.

Author Attribution

Peter Lam, the Master's candidate, performed most of the experimental work mentioned in this paper. Dr. Yupeng Chen was the principal investigator that led the scientific direction of the thesis along with providing guidance on the *in vivo* studies. Dr. Qian Chen and Dr. Michael Ehrlich provided guidance as well with their expertise in the field. Dr. Hongchuan Yu collaborated on the project and synthesized the rosette nanotubes used throughout the project. Dr. Philip McClure and Scott McAllister collaborated on the project as well for the *in vivo* study assessing the efficacy of the nanomatrix.